THE JOURNAL OF PHYSICAL CHEMISTRY B LETTERS

2005, *109,* 8557−8561
Published on Web 04/20/2005

Fourth-Order Raman Spectroscopy of Wide-Band Gap Materials

Satoru Fujiyoshi,*,†,§ Taka-aki Ishibashi,‡,§ and Hiroshi Onishi†,§

Department of Chemistry, Faculty of Science, Kobe University, Nada, Kobe, 657-8501 Japan, Department of Chemistry, Graduate School of Science, Hiroshima University, Kagamiyama, Higashi-Hiroshima, 739-8526 Japan, and Core Research for Evolutional Science and Technology, Japan Science and Technology Agency, Honmachi, Kawaguchi, 332-0012, Japan

Received: March 8, 2005; In Final Form: March 31, 2005

Low-frequency surface vibrations were observed on a rutile TiO_2(110) surface covered with trimethyl acetate (TMA) by using fourth-order Raman spectroscopy. The TMA-covered surface interfaced to air was irradiated with 18-fs light at a wavelength of 630 nm. A pump pulse excited vibrational coherence of Raman-active modes and a probe pulse interacts with the coherently excited surface to generate second harmonic light (315 nm), the intensity of which oscillated as a function of the pump−probe delay. Four bands were recognized at 180, 357, 444, and 826 cm^{-1} in the Fourier transformation spectrum of the oscillation and assigned to bulk phonons modified by the presence of the surface boundary condition. The Raman transition for the pump was nonresonant to the band gap excitation of TiO_2, as evidenced by the oscillation phase relative to the pump irradiation and by the oscillation amplitude as a function of the pump power. The observable range of this surface-selective spectroscopy is extended to wide-band gap materials on which one-photon resonance enhancement of the Raman-pump efficiency cannot be expected.

1. Introduction

Low-frequency vibrations play an essential role in dynamic phenomena on solid surfaces. Lattice vibrations of surface atoms are important in dissipation of the energy released in surface reactions. Large-amplitude motions of atoms are excited along the vibrational coordinate of frustrated rotations or frustrated translations. Transport of atoms and molecules is thus initiated with the multiple excitation of those modes. Rich information about those vibrational modes is provided by helium atom scattering[1] and electron energy-loss spectroscopy[2] when surfaces are examined in an ultrahigh vacuum (UHV). Fourth-order Raman (FR) spectroscopy[3−6] has recently been developed to observe the low-frequency modes of interfaces buried in a vapor, liquid, or solid environment.

Figure 1 illustrates the optical transitions employed in the FR spectroscopy.[5] An interface is irradiated with a femtosecond pump pulse of a frequency Ω. When the bandwidth of the pump pulse is broader than the energy difference between the vibrational ground (g) and excited (v) states of Raman-active modes, the vibrational coherence of the surface is excited via an impulsive stimulated Raman scattering (ISRS) process. At a time delay of t_d, a probe pulse of the frequency Ω interacts with the coherently excited vibrations to generate the second harmonic (SH) light pulse of 2Ω frequency. The pump-and-probe process contains four incident electric fields and the signal field E_{fourth} is proportional to a fourth-order response, $\chi^{(4)}$. The

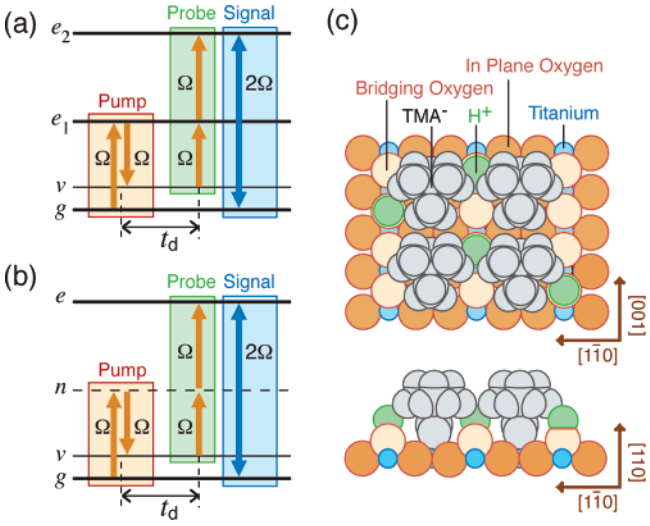

Figure 1. Energy diagrams of the fourth-order Raman (FR) spectroscopy (a) one-photon resonant and (b) nonresonant to an electronic excitation. When the bandwidths of the light pulses are broader than a vibrational wavenumber of a mode, ω_v, the FR signal of the mode can be observed. (c) The structure of the TMA-covered rutile TiO_2(110) surface.

even order spectroscopy offers an interface-selective observation of surface vibrations. The time-evolution of the 2Ω light is given by the sum of periodic oscillation

$$E_{fourth}(t_d, 2\Omega) \propto \chi^{(4)}(t_d) \propto \sum_v A_v \cos(\omega_v t_d + \varphi_v) \exp(-t_d/T_v) \quad (1)$$

where A_v, ω_v, φ_v, and T_v are the amplitude, frequency, phase,

* Corresponding author. E-mail: fujiyoshi@phys.titech.ac.jp. Present address: Department of Physics, Tokyo Institute of Technology, Meguro, Tokyo 152-8551, Japan.
† Kobe University.
‡ Hiroshima University.
§ Japan Science and Technology Agency.

10.1021/jp051203i CCC: $30.25

and dephasing time of each vibrational mode. This time-domain response $\chi^{(4)}(t_d)$ can be converted to a frequency-domain spectrum $\chi^{(4)}(\omega_v)$ via Fourier transformation (FT) analysis. Low-frequency vibrations are thereby observed with pump and probe pulses of visible[5] or near-infrared light.[3,4,6]

In reported examples of GaAs,[3] Cs on Pt,[4] Gd on W,[6] and an organic dye solution,[5] the pump light energy was tuned to be resonant with an electronic transition ($e_1 \leftarrow g$ and $v \leftarrow e_1$) at the interfaces to enhance the Raman-pump efficiency ($v \leftarrow e_1 \leftarrow g$) in Figure 1a. In the present work, the observable range of FR spectroscopy was extended to wide-band gap materials transparent to visible light, on which the one-photon resonance enhancement cannot be expected (Figure 1b). A rutile TiO_2(110) surface covered with an organic compound (trimethyl acetate, TMA) was irradiated with pump and probe pulses at a wavelength of 630 nm and oscillation was observed in the SH intensity. The FT spectrum represented low-frequency modes at the surface, because the FR transition is forbidden in the bulk rutile of D_{4h} symmetry. The band gap of rutile, 3.0 eV for the bulk[7] and 3.4 eV on the (110) surface,[8,9] was larger than the photon energy (2.0 eV). The oscillation phase relative to the pump irradiation, and the oscillation amplitude as a function of the pump power evidenced the nonresonant Raman-pump of the vibrational coherence. The closely packed monolayer of TMA (Figure 1c) was employed to protect the atomically flat surface of the metal oxide against air exposure and also to be a starting point for surface modification. The TMAs can later be substituted by larger carboxylates, such as retinoate[10] and a fluorescein derivative,[11] when immersed into an acetone solution of the substituting compound.

2. Experimental Section

A rutile TiO_2(110) surface covered with TMA monolayer (Figure 1c) was chosen as sample stable in air. An atomically flat TiO_2 surface prepared in an UHV is protected against air-exposure by the (2 × 1)-ordered monolayer of TMAs.[10,11] A one-side polished TiO_2(110) wafer (15 × 10 × 1 mm^3, Earth Chemicals) was Ar-ion sputtered at room temperature (RT) and annealed at 1000 K in a vacuum of 2×10^{-9} Torr. The sputter-annealed wafer was slightly reduced to be light blue in color and exhibited the (1 × 1) pattern in low-energy electron diffraction. A (2 × 1)-ordered monolayer of TMA was prepared by exposing the surface to trimethyl acetic acid vapor of 1×10^{-5} Torr for 60 s at RT. The TMA-covered surface was removed from the chamber and put on an open sample stage of the FR spectrometer operated in air.

The spectrometer is based on a sub-20-fs laser system.[5,12−14] Pump and probe pulses were generated in a noncollinear optical parametric amplifier (TOPAS-*white*, Quantronix) pumped by a Ti:sapphire regenerative amplifier (Hurricane, Spectra Physics) operated at 1 kHz. The wavelength of the pulses was set at 630 nm to be two-photon resonant to the band gap excitation of the TiO_2(110) surface.[8,9] The *p*-polarized pump pulse (14 mJ cm^{-2}) and *p*-polarized probe pulse (6 mJ cm^{-2}) were focused on the surface with the crossing angle of 2° and the incident angle θ of 50°. The incident plane of the beams was parallel to the [001] direction. The spot diameter of the beams was 0.15 mm. The *p*-polarized reflected 2Ω light was detected with a photomultiplier tube, whereas the reflected probe light of the frequency Ω was blocked with a short-wavelength-pass filter. The output of the photomultiplier was gated with a boxcar integrator, A/D converted, and sent to the computer on a pulse-to-pulse basis. The pump pulse was modulated at 500 Hz with a synchronous mechanical chopper. The signals with pump-on and pump-off were separately accumulated and the former was divided by the latter. Each data point was obtained by averaging over 36 000 probe pulses.

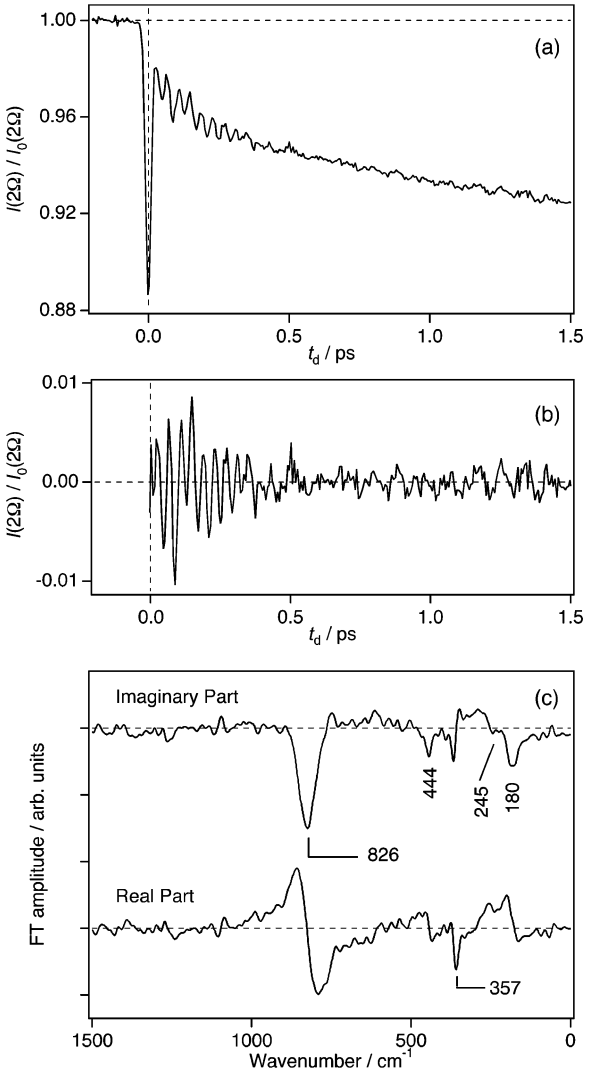

Figure 2. (a) Intensity change of the reflected 2Ω light of the TMA-covered TiO_2(110) surface. (b) The oscillatory component of the fourth-order Raman (FR) signal. (c) The imaginary part and the real part of the FT spectrum of the oscillation.

The full width at half-maximum (fwhm) of the intensity cross-correlation function of the pump and probe pulses (τ_{cc}) was determined to be 26 fs by using a SH signal from a 50-μm-thick β-BaB_2O_4 crystal. The fwhm of the pump and probe pulses (τ_{pu} and τ_{pr}) was estimated to be 18 fs on the assumption that the shapes of these pulses were a Gaussian function. The time origin was determined to an accuracy of 3 fs by using the SH signal of the pump and probe pulses on the TiO_2(110) surface.

3. Results and Discussion

The intensity of the 2Ω light of the TiO_2(110) surface, $I(2\Omega)$, was modulated by the pump pulse. Figure 2a shows $I(2\Omega)/I_0(2\Omega)$ as a function of the pump−probe delay, where $I_0(2\Omega)$ is the pump-free intensity of 2Ω light.[15] A sharp, negative peak at the time origin ($t_d = 0$) was followed by a decay over 1 ps. Periodic modulations superposed on the decay reflect surface atom vibrations due to the FR response (eq 1).

The sharp peak is assigned to the electronic response of the surface irradiated by the pump pulse, and reproduced with a Gaussian function having a fwhm of 23 fs. The width narrower

than τ_{cc} represented the instrumental response when the electronic response is assumed to be instantaneous. The relative intensity of 2Ω-light is given by

$$\frac{I(t_d, 2\Omega)}{I_0(2\Omega)} = \frac{|E_0(2\Omega) + E_S(t_d, 2\Omega)\exp(i\phi)|^2}{|E_0(2\Omega)|^2} \quad (2)$$

where $E_0(2\Omega)$ denotes the reflected 2Ω field generated at the pump-free surface and $E_S(t_d, 2\Omega)$ represents the pump-induced signal field including the negative peak, the decay, and the oscillation attributed to the FR response. ϕ gives the relative phase of $E_S(t_d, 2\Omega)$ and $E_0(2\Omega)$. When $|E_0| \gg |E_S|$, eq 2 is approximated as

$$\frac{I(t_d, 2\Omega)}{I_0(2\Omega)} = 1 + \frac{2E_0(2\Omega)\,E_S(t_d, 2\Omega)\cos\phi}{I_0(2\Omega)} \quad (3)$$

Equation 3 shows that $E_S(t_d, 2\Omega)$ is heterodyned to make the periodic oscillation of $I(t_d, 2\Omega)$, i.e., the FR signal in the time domain.[5] The oscillation amplitude is therefore linearly proportional to the material response. This makes a contrast with a sum-frequency signal, which is produced in a homodyne optical process to be proportional to the squared material response.[16] Assuming the dephasing time of the two-photon resonant state (e) is much shorter than the pulse duration of the probe pulse (τ_{pr}), the pulse envelope of $E_0(t, 2\Omega)$ as a function of t is linearly proportional to that of the squared probe field. The second term on the right-hand side of eq 3 is approximated as

$$E_0(2\Omega)E_S(t_d, 2\Omega) \propto \int_{-\infty}^{\infty} dt_2 |E_{pr}(t_2 - t_d, \Omega)|^4 \times \int_{-\infty}^{t_2} dt_1 |E_{pu}(t_1, \Omega)|^2 \chi^{(4)}(t_2 - t_1) \quad (4)$$

where E_{pr} and E_{pu} denote the probe and pump fields, respectively. Equation 4 indicates that the instrumental response is given by the temporal profile of the pump intensity convoluted with that of the squared probe intensity, whereas τ_{cc} is proportional to the fwhm of the simple convolution of the pump and probe intensities. The fwhm of the instrumental response was estimated to be 23 fs by τ_{pu}, τ_{pr}, and eq 4. The estimated width of the instrumental response agrees with the width of the electronic response (23 fs).

The subsequent decay was fitted in the range of 0−3 ps to extract the oscillation. A double exponential function having time constants of $\tau_1 = 0.21$ ps and $\tau_2 = 4.4$ ps reproduced the observed profile.[17] The oscillation in Figure 2b was obtained by subtracting the electronic response and the double exponential decay. Figure 2c presents the real and imaginary parts of the FT spectrum of the oscillation. To smooth the FT spectrum, the oscillation at 0−3 ps was multiplied by a window function, a Gaussian function with a half width at half-maximum (hwhm) of 1 ps centered at $t_d = 0$ ps, and zero data points were added at 3−30 ps. This operation with the window function determined the wavenumber resolution of the FT spectrum. Multiplying the window function corresponds to convolving the FT spectrum with a Gaussian function having a fwhm of 15 cm^{-1}. On the other hand, the relative sensitivity at different wavenumbers was given by the Fourier transformation of the instrumental response function (a Gaussian function having a fwhm of 23 fs).[18−20] The sensitivity curve thereby calculated was a Gaussian function centered at 0 cm^{-1} with a hwhm of 650 cm^{-1}. The FT spectrum in Figure 2c was not corrected by the sensitivity.

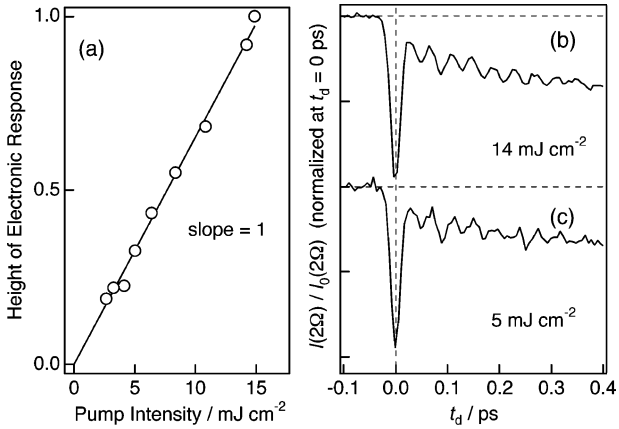

Figure 3. (a) Intensity of the electronic response at $t_d = 0$ as a function of the pump power. The oscillation amplitude normalized to the intensity of the electronic response is presented for two extreme pump powers, (b) 14 and (c) 5 mJ cm^{-2}.

Four bands were recognized at 180, 357, 444, and 826 cm^{-1} in the FT spectrum of Figure 2c accompanied with a shoulder at 245 cm^{-1}. The first band appeared at the position of an IR-active, bulk phonon mode of E_u symmetry (183 cm^{-1}).[21] The wavenumbers of the third and fourth bands agreed with that of Raman-active bulk phonons, an E_g-symmetry mode (447 cm^{-1}) and a B_{2g}-symmetry mode (826 cm^{-1}).[22] The cross section of the FR scattering is proportional to the product of a Raman tensor in the pump transition and a hyper-Raman tensor in the probe transition.[5] In the bulk medium having a D_{4h} symmetry, a Raman-active mode is inactive for a hyper-Raman transition.[23] Hence, the FR transition of the observed bands at 180, 444, and 826 cm^{-1} is forbidden in the bulk rutile and allowed at the surface where the centrosymmetry is broken. The wavenumbers of surface phonons determined in the present study reproduced those of bulk phonons in the literature, indicating that the bulk modes are only slightly modified by the presence of the surface boundary condition. In electron energy loss studies on TMA-free TiO_2(110),[24,25] surface phonon bands were found at 353−370, 418−434, and 756−772 cm^{-1}, which was consistent with the present results.

The shape of the three bands at 180, 444, and 826 cm^{-1} was symmetric in the imaginary part and dispersive in the real part of the FT spectrum. This tells us the phase of the vibrational coherence relative to the pump irradiation; sine-like oscillation of atoms was coherently pumped at $t_d = 0$, i.e., $\varphi_v = 3\pi/2$ in eq 1.[26] On the other hand, cosine-like oscillation with $\varphi_v = 0$ or π was observed on GaAs,[3] Cs on Pt,[4] Gd on W,[6] and the dye solution,[5] where vibrational coherence was pumped by one-photon resonant transitions. The phase shift from a cosine function to a sine function was evidence of the nonresonant Raman-pump on our TMA-covered TiO_2. A similar phase shift of vibrational coherence has been known in third-order Raman spectroscopy based on ISRS, an established bulk-sensitive method, where vibrational coherence was Raman-pumped and detected by transmission[27] or reflection[12] of probe pulse. The oscillation appearing on the transmitted or reflected probe intensity is expressed as a sum of cosine functions when the pump transition is one-photon resonant.[12,18,28] Sine-like oscillation is created with pump pulses nonresonant to a one-photon transition between electronic states.[12,18,28−31]

Figure 3 shows the oscillation amplitude as a function of the pump power. The height of the electronic response at $t_d = 0$ was linearly increased with the pump intensity of 0−15 mJ cm^{-2} in panel a. The time-domain responses observed with the pump pulses of the two extreme intensities (14 and 5 mJ cm^{-2}) are

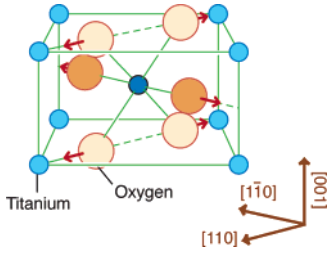

Figure 4. Atom displacements of B_{1g} bulk phonon of rutile.

compared in panels b and c. The oscillation amplitude relative to the negative peak height was identical to the two responses. The FR oscillation amplitude was therefore linearly proportional to the pump intensity. The result confirmed that the FR signal is proportional to the expected fourth-order Raman process shown in Figure 1b. If the observed phonon modes had been resonantly excited by the band gap excitation due to two-photon absorption, the amplitude would have been proportional to the squared pump intensity. This was not the case.

The hyper-Raman transition in probing the excited coherence was two-photon resonant to the band gap excitation of the (110) surface. The efficiency of the SH signal was measured on a TMA-free TiO_2(110) surface exposed to air with excitation wavelengths of 850−650 nm.[9] A sharp rise of the SH intensity due to the two-photon resonance with the surface band gap (3.4 eV) was observed at 730 nm. A theoretical study[32] revealed that −Ti−O−Ti− zigzag chains of 6-fold coordinated titanium atoms and bridge oxygen atoms dominantly contribute to the polarization to generate the SH light. Our excitation wavelength, 630 nm, exceeded the threshold of the two-photon resonance. The pump-free 2Ω-light, $I_0(2\Omega)$, was due to two-photon resonant SH signal (see note 15). Thus, the probe process was attributed to the two-photon resonant hyper-Raman process of the (110) surface.

The most intense 826-cm^{-1} band was broader than the other three. That band was assigned to the B_{2g}-symmetry mode of the bulk phonon affected by the presence of the surface boundary condition. The symmetric peak in the imaginary part of the FT spectrum was well-fitted with a Gaussian function rather than with a Lorenz function. The bandwidth deconvoluted to 56 cm^{-1} by considering the instrumental resolution (15 cm^{-1}), being twice as broad as the bandwidth of the bulk B_{2g} mode (25 cm^{-1}).[22] The broadened band can best be understood with an eigen frequency distribution in the observed portion of the (110) surface. Figure 4 illustrates the displacements of bulk atoms caused by the B_{2g}-mode excitation.[33,34] When projected to a TMA-free (110) surface, that mode contains the motion of bridge oxygen atoms perpendicular to the surface plane. The presence of the surface possibly perturbs this motion so that the surface mode localized at the topmost layer splits from the bulk phonon band. In addition, our TiO_2 surface was covered with a monolayer of TMAs. The equivalent number of hydrogen atoms were provided to the surface in the dissociative adsorption of the parent acid. They were adsorbed on top of the bridge oxygen atoms.[35] The proton and TMA can further perturb the localized mode at the topmost layer. Future studies with the TiO_2 surface covered with different carboxylates are required to assign the origin of the broadening. Comparison with low-frequency modes theoretically predicted on the TMA-free surface[36] is also demanded.

Heterogeneity of the adsorbed TMAs is a less probable origin of the broadening of the 826-cm^{-1} band. TMAs are homogeneously chemisorbed on the TiO_2 surface where each TMA anion is bound to a pair of Ti cations.[37] The TMA-covered surface is terminated with bulky, hydrophobic *t*-butyl groups, and they remain intact when exposed to air[10] or liquid acetone.[11] However, the band gap excitation by two-photon absorption may possibly cause the photochemical degradation of TMAs. Irregular structures of the TiO_2 surface (steps, oxygen vacancies, and different surface phases) are the other possible origins of the heterogeneity. The number of those irregularities is about a few percent on similarly prepared surfaces.[38,39] That number is less than required to cause the significant broadening.

The origin of the FR band at 357 cm^{-1} is unknown. Bulk phonon modes are missing in corresponding wavenumbers.[21,22] The wavenumber of the FR band agreed with one of surface optical phonon (Fuchs-Kliewer) modes at 370[27] and 353[24,25] cm^{-1} on the TMA-free TiO_2(110) surface. On the other hand, the shape of the 357-cm^{-1} band was dispersive in the imaginary part and symmetric in the real part of Figure 2c. A cosine-like oscillation with respect to the pump irradiation and hence a different excitation mechanism are suggested to that mode of vibration. On an AlGaAs/GaAs heterojunction, cosine-like oscillation of AlGaAs due to the vibrational coherence was observed in the nonresonant condition of AlGaAs.[40]

In summary, surface lattice vibrations were coherently excited on the TMA-covered TiO_2(110) surface irradiated with an ultrashort light pulse out of one-photon resonance of the band gap transition. The excited coherence was probed in the oscillatory modulation of the signal intensity of a frequency 2Ω. Wide-band gap materials transparent even to visible light are now in the observable range of fourth-order Raman spectroscopy, a unique method detecting low-frequency vibrations at buried interfaces.

Note Added after ASAP Publication. This letter was released ASAP on April 20, 2005 with an incorrect author affiliation and some minor errors in eq 1 and the Results and Discussion section. The corrected version was reposted on April 21, 2005.

References and Notes

(1) Hofmann, F.; Toennies, J. P. *Chem. Rev.* **1996**, *96*, 1307.
(2) Henrich, V. E.; Cox, P. A. *The Surface Science of Metal Oxides*; Cambridge University Press: New York, 1994; Chapter 3.
(3) Chang, Y. M.; Xu, L.; Tom, H. W. K. *Phys. Rev. Lett.* **1997**, *78*, 4649
(4) Watanabe, K.; Takagi, N.; Matsumoto, Y. *Chem. Phys. Lett.* **2002**, *366*, 606
(5) Fujiyoshi, S.; Ishibashi, T.; Onishi, H. *J. Phys. Chem. B* **2004**, *108*, 10636
(6) Bovensiepen, U.; Melnikov, A.; Radu, I.; Krupin, O.; Starke, K.; Wolf, M.; Matthias, E. *Phys. Rev. B* **2004**, *69*, 235417.
(7) Grant, F. A. *Rev. Mod. Phys.* **1959**, *31*, 646.
(8) Kobayashi, E.; Mizutani, G.; Ushioda, S. *Jpn. J. Appl. Phys.* **1997**, *36*, 7250.
(9) Kobayashi, E.; Wakasugi, T.; Mizutani, G.; Ushioda, S. *Surf. Sci.* **1998**, *402*−*404*, 537.
(10) Ishibashi, T.; Uetsuka, H.; Onishi, H. *J. Phys. Chem. B* **2004**, *108*, 17166.
(11) Pang, C. L.; Ishibashi, T.; Onishi, H. *Jpn. J. Appl. Phys.* in press.
(12) Fujiyoshi, S.; Ishibashi, T.; Onishi, H. *J. Phys. Chem. B* **2004**, *108*, 1525.
(13) Fujiyoshi, S.; Ishibashi, T.; Onishi, H. *J. Phys. Chem. A* **2004**, *108*, 11165.
(14) Fujiyoshi, S.; Ishibashi, T.; Onishi, H. *J. Mol. Struct.* **2005**, *735*−*736*, 169.
(15) $I_0(2\Omega)$ was due to the two-photon-resonance SH signal of the rutile TiO_2(110) surface. It was a reflected *p*-polarized 2Ω-light generated in only the *p*-polarized probe pulse [001] direction. The intensity of the *p*-polarized 2Ω light in the [001] direction, $I_0(2\Omega)$, was 16 times larger than that in the [110] direction. The *p*-polarized 2Ω light generated from the *p*-polarized probe light (P_{in}/P_{out}) in the [001] direction, $I_0(2\Omega)$, was more than one thousand times larger than the *s*-polarized 2Ω light generated from the *p*-polarized probe light (P_{in}/S_{out}) in the same direction. The dependence of the direction and polarization is identical with that of the two-photon

resonant SH signal of the TiO_2(110) surface reported from Kobayashi et al.[8,9] Thus, the observed SH signal of $I_0(2\Omega)$ was due to the second-order nonlinear response of rutile TiO_2(110) surface on the two-photon resonance. $I_0(2\Omega)$ was ~2000 photons per pulse (probe intensity: 6 mJ cm^{-2}; spot diameter: 0.15 mm).

(16) Shen, Y. R. *The Priciple of Nonlinear Optics*; Wiley-Interscience: New York, 1984.

(17) The time constants of τ_2 was predetermined by using the signal of 3−100 ps before the fitting analysis of τ_1. The assignments of the components ($\tau_1 = 0.21$ ps and $\tau_2 = 4.4$ ps) are not definite. The responses of TiO_2 particles with a decay constant similar to τ_1 and τ_2 have been observed. The faster response was assigned to the trapping time of photoexcited electrons,[41,42] and the slower response was assigned to the electron−hole recombination.[43] The responses observed in the present work may relate to similar dynamics of the generated electrons and holes. Further experiment involving pump intensity dependence and the SH spectrum of the components[44] would lead to conclusive results.

(18) Ziegler, L. D.; Fan, R.; Desrosiers, A. E.; Scherer, N. F. *J. Chem. Phys.* **1994**, *100*, 1823.

(19) Cho, M.; Du, M.; Scherer, N. F.; Fleming, G. R.; Mukamel, S. *J. Chem. Phys.* **1993**, *99*, 2410.

(20) Fujiyoshi, S.; Takeuchi, S.; Tahara, T. *J. Phys. Chem. A* **2003**, *107*, 494.

(21) Eagels, D. M. *J. Phys. Chem. Solids* **1964**, *25*, 1243.

(22) Porto, S. P. S.; Fleury, P. A.; Damen, T. C. *Phys. Rev.* **1967**, *154*, 522.

(23) Long, D. A. *Raman Spectroscopy*; McGraw-Hill Inc.: New York, 1977.

(24) Rocker, G.; Schaefer, J. A.; Göpel, W. *Phys. Rev. B* **1984**, *30*, 3704.

(25) Cox, P. A.; Egdell, R. G.; Eriksen, S.; Flavell, W. R. *J. Electron Spectrosc. Relat. Phenom.* **1986**, *39*, 117.

(26) The uncertainty of the time origin of the temporal profiles, 3fs, determines those of the phase of the vibrational bands. The estimated values were 0.03 π, 0.07 π, 0.08 π, and 0.15 π for the bands at 180, 357, 444, and 826 cm^{-1}, respectively.

(27) Dhar, L.; Rogers, J. A.; Nelson, K. A. *Chem. Rev.* **1994**, *94*, 157.

(28) Nagasawa, Y.; Watanabe, A.; Takikawa, H.; Okada, T. *J. Phys. Chem. A* **2003**, *107*, 632.

(29) McMorrow, D.; Lotshaw, W. T. *J. Phys. Chem.* **1991**, *95*, 10395.

(30) Vöhringer, P.; Scherer, N. F. *J. Phys. Chem.* **1995**, *99*, 2684.

(31) Matsuo, S.; Tahara, T. *Chem. Phys. Lett.* **1997**, *264*, 636.

(32) Sato, H.; Mizutani, G.; Wolf, W.; Podloucky, R. *Phys. Rev. B* **2004**, *70*, 125411.

(33) Samara, G. A.; Peercy, P. S. *Phys. Rev. B* **1973**, *7*, 1131.

(34) Lee, C.; Ghosez, P.; Gonze, X. *Phys. Rev. B* **1994**, *50*, 13379.

(35) Sayago, D. I.; Polcik, M.; Lindsay, R.; Toomes, R. L.; Hoeft, J. T.; Kittel, M.; Woodruff, D. P. *J. Phys. Chem. B* **2004**, *108*, 14316.

(36) Harrison, N. M.; Wang, X.-G.; Muscat, J.; Scheffler, M. *Faraday Discuss.* **1999**, *114*, 305.

(37) Henderson, M. A.; White, J. M.; Uetsuka, H.; Onishi, H. *J. Am. Chem. Soc.* **2003**, *125*, 14974.

(38) Onishi, H.; Iwasawa, Y. *Bull. Chem. Soc. Jpn* **1995**, *68*, 2447.

(39) Fukui, K.; Onishi, H.; Iwasawa, Y. *Phys. Rev. Lett.* **1997**, *79*, 4202.

(40) Chang, Y. M.; Chang, N. A. *J. Appl. Phys.* **2003**, *93*, 2015.

(41) Skinner, D. E.; Colombo, D. P.; Cavaleri, J. J.; Bowman, R. M. *J. Phys. Chem.* **1995**, *99*, 7853.

(42) Iwata, K.; Takaya, T.; Hamaguchi, H.; Yamakata, A.; Ishibashi, T.; Onishi, H.; Kuroda, H. *J. Phys. Chem. B* **2004**, *108*, 20233.

(43) Colombo, D. P.; Roussel, K. A.; Saeh, J.; Skinner, D. E.; Cavaleri, J. J.; Bowman, R. M. *Chem. Phys. Lett.* **1995**, *232*, 207.

(44) Yamaguchi, S.; Tahara, T. *J. Phys. Chem. B* **2004**, *108*, 19079.